minerals

MDPI

Article

Influence of Temperature on the Formation of Ag Complexed in a $S_2O_3^{2-}$–O_2 System

Aislinn M. Teja-Ruiz [1], Julio C. Juárez-Tapia [1,*], Leticia E. Hernández-Cruz [1], Martín Reyes-Pérez [1], Francisco Patiño-Cardona [2], Ivan A. Reyes-Dominguez [3], Mizraim U. Flores-Guerrero [4] and Elia G. Palacios-Beas [5]

1 Área Académica de Ciencias de la Tierra y Materiales, Universidad Autónoma del Estado de Hidalgo (UAEH), Pachuca de Soto 42184, Mexico; ice9791@gmail.com (A.M.T.-R.); lesperanza.hernandez@gmail.com (L.E.H.-C.); mar_77_mx@hotmail.com (M.R.-P.)
2 Ingeniería en Energía, Universidad Politécnica Metropolitana de Hidalgo, Tolcayuca 43860, Mexico; franpac@terra.com.mx
3 Catedrático CONACYT-Instituto de Metalurgia, Universidad Autónoma de San Luis Potosí, San Luis Potosi 78210, Mexico; ivanalejandro2001@hotmail.com
4 Área de Electromecánica Industrial, Universidad Tecnológica de Tulancingo, Tulancingo 43642, Mexico; uri_fg@hotmail.com
5 Escuela superior en Ingeniería Química e Industrias Extractivas (ESIQIE), Instituto Politécnico Nacional (IPN), Zacatenco 07738, Mexico; epalacios@ipn.mx
* Correspondence: jcjuarez@uaeh.edu.mx; Tel.: +52-771-717-2000 (ext. 2279)

Academic Editor: Karen Hudson-Edwards
Received: 24 October 2016; Accepted: 24 January 2017; Published: 27 January 2017

Abstract: Metallic elements of higher economic value, occurring in the mineralogy of Zimapán, are Pb, Zn, Cu, and Fe; said elements are sold as concentrates, which, even after processing, generally include significant concentrations of Mo, Cd, Sb, Ag, and As that can be recovered through different leaching methods. In this work, the influence of temperature in the complexation of silver contained in a concentrate of Zn using the technology of thiosulfate with oxygen injection was studied. Chemical and mineralogical characterization of the mineral concentrate from the state of Hidalgo, Mexico confirmed the existence of silver contained in a sulfide of silver arsenic ($AgAsS_2$) by X-ray Diffraction (XRD). The results obtained by Atomic Absorption Spectrophotometry (AAS) reported abundant metallic contents (% *w*/*w*) (48% Zn, 10.63% Fe, 1.97% Cu, 0.84% Pb, 0.78% As, and 0.25% Ag). These results corroborate the presence of metallic sulfides such as pyrite, chalcopyrite, and wurtzite; this last species was identified as the matrix of the concentrate by X-ray Diffraction (XRD) and Scanning Electron Microscopy-Energy-Dispersive X-ray Spectroscopy (SEM-EDS). Pourbaix diagrams were constructed for the $AgAsS_2$–$S_2O_3^{2-}$–O_2 system at different temperatures, which allowed the chemical reaction of leaching to be established, in addition to determining Eh-pH conditions in which to obtain silver in solution. The highest recoveries of the precious metal (97% Ag) were obtained at a temperature of 333 K and $[S_2O_3^{2-}]$ = 0.5 M. The formation of silver dithiosulfate complex ($Ag(S_2O_3)_2^{3-}$) was confirmed by the characterization of the leach liquors obtained from the experiments performed in the temperature range of 298 to 333 K using Fourier transform infrared spectroscopy (FTIR).

Keywords: silver; dissolution; thiosulfate; characterization; complex; temperature; arsenic

1. Introduction

Currently, the search for alternative leaching agents to traditional extraction processes is presented as an essential method for scientific and industrial interests to combat the disadvantages of cyanidation. The limited selectivity and high toxicity involved in the use of cyanide have directed efforts in different

research fields to use leachates such as thiourea (CH_4N_2S), thiocyanates (SCN^-), and thiosulfate ($S_2O_3^{2-}$) [1]—processes which have achieved profitable recoveries with lesser ecological impacts [2].

Thiosulfate ($S_2O_3^{2-}$) is one of the most promising reagents for the leaching of precious metals [3]. It has been shown that by maintaining sufficient concentrations of thiosulfate, ammonia, copper, and oxygen in the solution, under suitable Eh-pH conditions, precious metals such as gold can be easily extracted with a low consumption of reagents [4]. In the last decade, recoveries with thiosulfate have been optimized through the use of oxidizing agents such as oxygen (O_2), and the addition of metal ions with catalytic character have reached recoveries up to 97.13% Ag (I) in $S_2O_3^{2-}$-O_2-Zn^{2+}, at 0.25 M $S_2O_3^{2-}$ concentration, an oxygen partial pressure of 1 atm, and temperature of 318 K over four hours [5].

Leaching from sulphurous ores using thiosulphate ($S_2O_3^{2-}$) involves a complicated chemical reaction which requires a comprehensive thermodynamic analysis prior to experimental tests in order to determine the conditions in which precious metals are solubilized even in presence of other metals contained in the system. Some studies have clarified the dissolution chemistry of leaching systems by calculating the distribution of species and making Pourbaix diagrams that determine the ratios between ore concentrations and reagents [6], in addition to performing thermodynamic calculations that show the favorable recovery of silver (Ag), in which the conditions of the complex formed with the leaching agent are stable in solution [7].

This study shows the characterization of concentrated Zn from Zimapán, of which the particles were bounded to 74 microns and subjected to a leaching process in a $S_2O_3^{2-}$–O_2 system in order to study the influence of temperature on the formation of complexed silver.

2. Materials and Methods

Prior to experimental tests, zinc ore concentrate from the mining district of Zimapán in Hidalgo, Mexico was dried and homogenized in order to obtain a representative sample. Later, it was analyzed using the atomic absorption spectrophotometry (AAS) technique using a Perkin Elmer-Analyst 200 spectrophotometer in order to identify and quantify the elements present in the zinc concentrate. Three samples of 1 g of each particle size (44, 53, and 74 μm) to which the mineral concentrate were sifted were digested with Aqua Regia (0.03 L of nitric acid (HNO_3)–0.01 L of hydrochloric acid (HCl)) at a temperature of 323 K, until the solids dissolved completely. The digested solution of each sample was filtered and measured at 0.1 L in order to determine the content of Ag and As in the concentrate of Zn by the technique of chemical analysis using atomic absorption spectrometry (AAS).

Morphological study of the representative sample was performed using X-ray Diffraction (XRD) with an INEL X-ray diffractometer, model EQUINOX 2000 (Thermo Fisher Scientific, Ecublens, Switzerland), with Co-Ka1 radiation (1.789010 Å) operating at 30 mA and 20 KV, a voltage of 220 V, and a full width at half maximum (FWHM) resolution of 0.095; and also the scanning electron microscopy-energy-dispersive X-ray spectroscopy (SEM-EDS) technique using a JEOL electron microscope, model JSM 6300 (JEOL, Tokyo, Japan), with a 30 KV voltage and a 21-mm field depth at different magnifications with secondary electrons, and backscattered in order to identify the mineralogical species present in the Zn concentrate powders.

According to the mineral species identified by the XRD silver complexing agent, and which was proposed for the leaching system ($S_2O_3^{2-}$), a thermodynamic simulation of the system was performed using two metallic elements (Ag and As) and three nonmetallic (S, H, and O_2), by building Pourbaix diagrams at different temperatures in order to establish a framework for the behavior of these elements in an aqueous system; HSC Chemistry software 5.11 (Outotec, Cleveland, OH, USA) was used.

In order to perform the silver dissolution, a glass reactor with a 500-mL capacity on a Thermo Scientific Super Nuova hot plate fitted with magnetic stirring was used; oxygen was then injected through a diffuser and regulated to 1 atm by a flowmeter with a 200 psi maximum capacity. A series of experiments were performed at different temperatures (298, 313, and 333 K), keeping all other parameters constant. The leaching process of Ag (I) was monitored by taking successive 10-mL aliquots

at different times, for 360 min, which were then analyzed usingAtomic Absorption Spectrometry (AAS). Leached liquors were characterized using Fourier transform infrared spectroscopy (FTIR) in order to confirm the formation of the silver-thiosulfate species using a Fourier transform infrared spectrometer model Tensor 27, Bruker (Bruker Optics Inc., Billerica, MA, USA), with a mid-infrared (MIR) source.

3. Results

3.1. Chemical Analysis Using Atomic Absorption Spectrometry (AAS)

Table 1 shows the analyzed elements in the Zn concentrate using the AAS technique; the obtained results determined a 0.25% (255 g·ton^{-1}) silver content. In addition, the presence of 48% Zn as a major component, followed by Fe and Cu concentrations, were detected. Sb, Pb, and Cd were identified as less-abundant elements in the concentrate. The graphical representation of the elemental analysis contained in the mineral sample is observed in Figure 1.

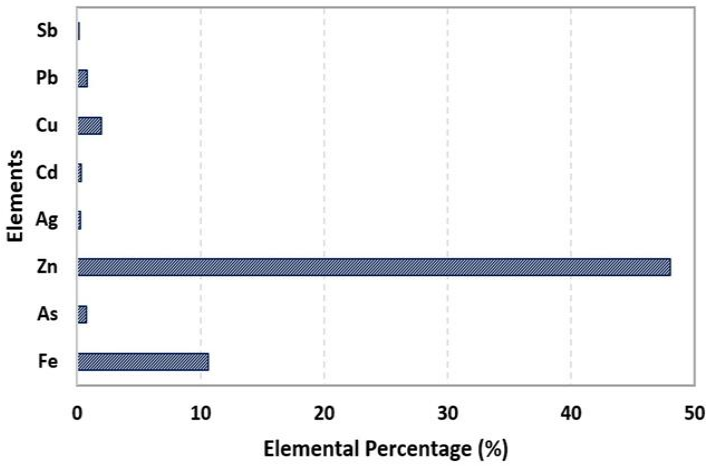

Figure 1. Average elemental composition of the concentrate of Zn.

Table 1. Chemical elemental analysis of the mineral concentrate.

Element	% *w*/*w*	R^2
Fe	10.63	0.9998
As	0.78	0.9996
Zn	48	0.9989
Ag	0.25	0.9998
Cd	0.33	0.9991
Cu	1.97	0.9998
Pb	0.84	0.9998
Sb	0.05	0.9987

In order to determine silver and arsenic contents, triple digestion of powders held in 200, 270, and 325 meshes of Tyler series were also performed. AAS analyses for these samples reported uniform silver content for all measured particle diameters in addition to high arsenic concentrations, as shown in Table 2.

Table 2. Ag and As content in Zn concentrate per mesh.

Mesh Number	Micrometers (μm)	Ag (g/ton)	As (g/ton)
200	74	255	541
270	53	253	846
325	44	228	952

3.2. Characterization by X-ray Diffraction (XRD)

Figure 2 shows a diffractogram obtained using X-ray diffraction, in which the following spectra corresponding to ore species are observed: wurtzite (ZnS [PDF: 00-391-363], identified as the ore matrix of this concentrate), and chalcopyrite ($CuFe_9S_{16}$) [PDF: 00-270-165]. The mineral species that contain the precious metal in the concentrate of Zn was identified as an argentiferous arsenic sulfide ($AgAsS_2$) [PDF: 00-431-406].

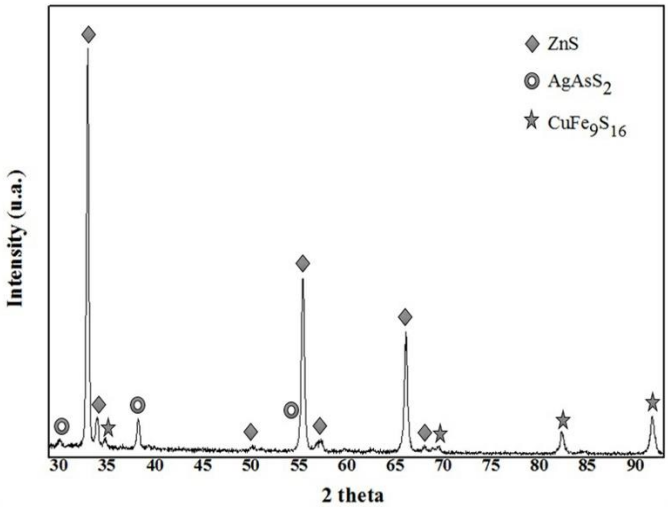

Figure 2. X-ray diffractogram of the powders of full-sized ore concentrate of Zn.

3.3. Characterization Using Scanning Electron Microscopy-Energy-Dispersive X-ray Microanalysis (SEM-EDS)

Figure 3, obtained with secondary electrons, reports that the heterogeneous morphology of the particles correspond to hemispherical and polygonal shapes with smooth angles. General EDS spectrum (Figure 4) reveals the elemental composition of the concentrate, which is consistent with chemical analysis using AAS, determining Zn, Cu, and Fe as main metal components of the sample powder.

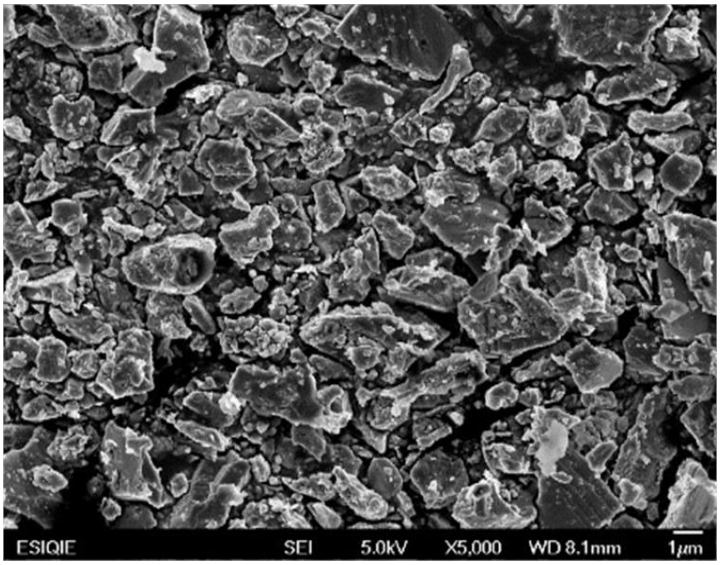

Figure 3. Micrograph of a powder sample of a Zn concentrate obtained using secondary electrons.

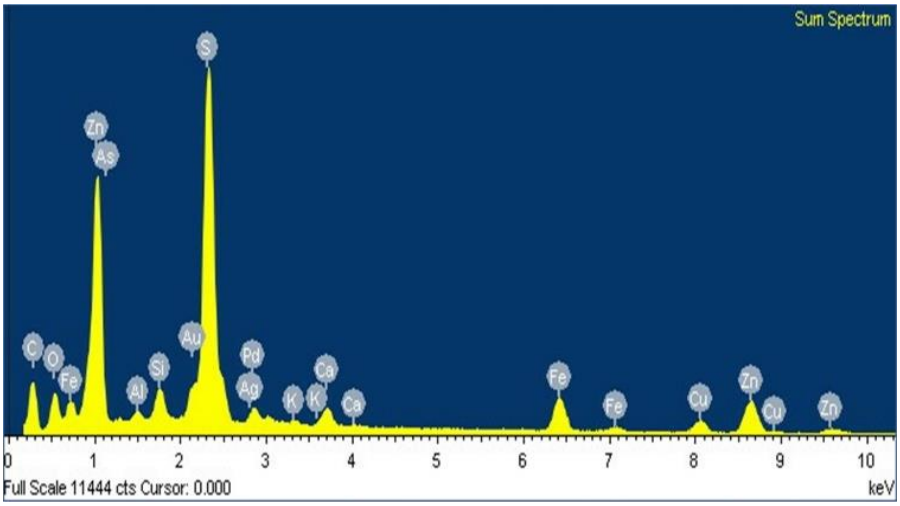

Figure 4. Energy-dispersive X-ray spectrum performed on an all-in-one powder sample of Zn concentrate.

Mapping was performed on the concentrate of Zn particles and is shown in Figure 5, which shows sulfur as the most abundant element in the sample, and is mainly related to metallic elements such as Zn, Fe, and Cu, suggesting the presence of mineral species, such as wurtzite (ZnS), pyrite (Fe_2S), and chalcopyrite ($CuFe_9S_{16}$).

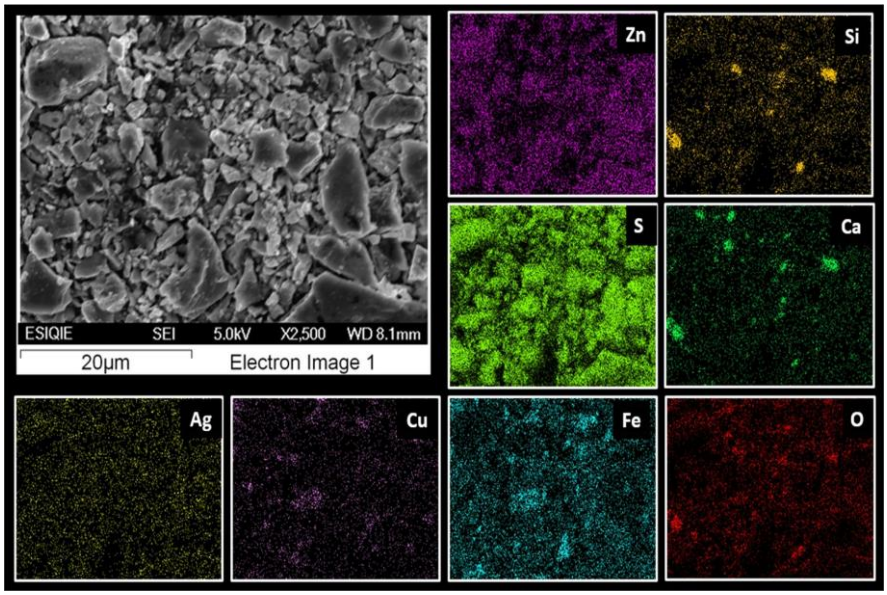

Figure 5. Mapping of concentrate Zn powders.

3.4. Thermodynamic Simulation of Ag (I) Dissolution

In the diagrams of experiments performed at different temperatures presented in Figures 6 and 7, we can see that the species $Ag(S_2O_3)_2^{3-}$ is obtained at pH = 9 and in the range of Eh = 0 to 1.3 volts. This corresponds to ion of Ag (I) complexed with the leaching agent, thereby confirming that the pH range is broad for dissolution compared to the short potential range.

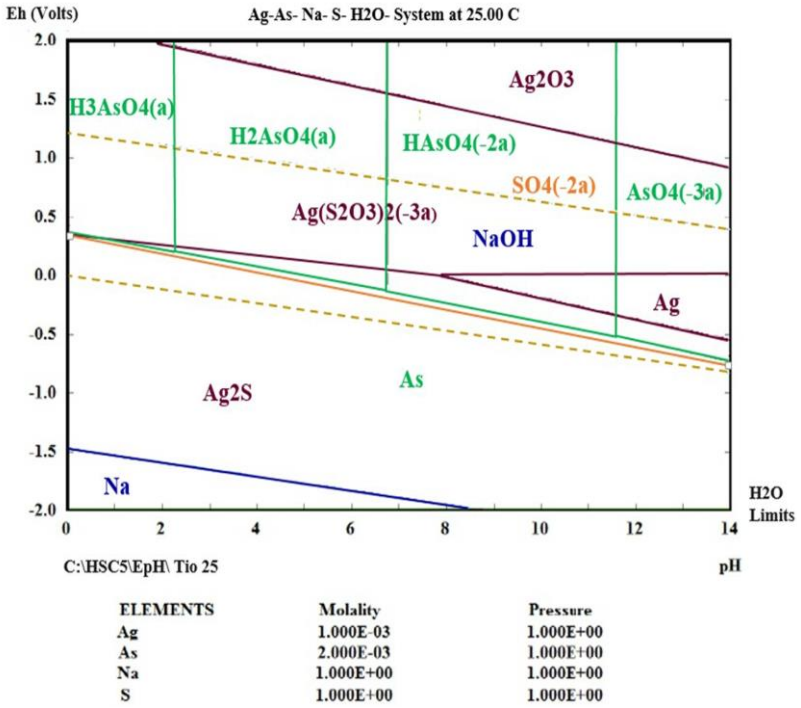

Figure 6. Diagram of the Eh-pH for the Ag–As–S–H_2O system at 298 K.

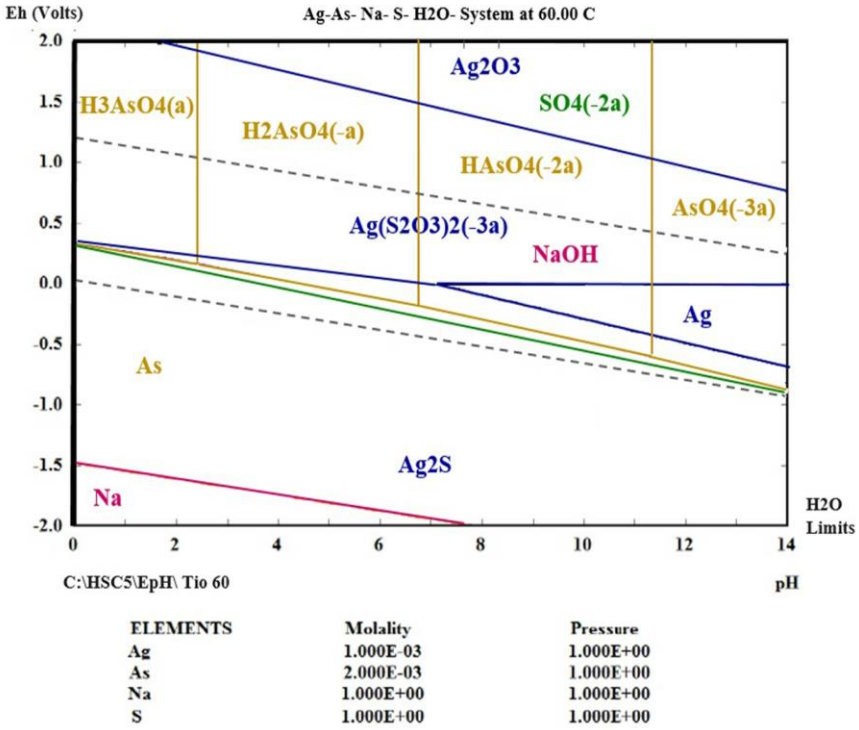

Figure 7. Diagram of the Eh-pH for the Ag–As–S–H_2O system at 313 K.

3.5. Dissolution of Ag (I) at Different Temperatures

The mesh with a more concentrated distribution of silver was selected (in this case, the 200 mesh) as an appropriate particle size to study the influence of temperature on the silver solution. Experimental conditions for the leaching of Ag (I) in the $S_2O_3^{2-}$–O_2 system are shown in Table 3.

Table 3. Experimental condition constants.

Constant Parameters	Measurement
Amount of mineral	40 $g \cdot L^{-1}$
$[S_2O_3^{2-}]$	0.5 M
Stirring speed	670 min^{-1}
pH	9
[NaOH]	0.1 M
Partial Oxygen Pressure	1 atm
Volume of Solution	500 mL

The graphical representation of the values obtained in the leaching experiments is shown in Figure 8, where it can be seen that as the temperature increases, the percentage of silver in the leached solution also increases.

With a temperature of 333 K, the conversion of silver is 0.978 in a reaction time of 360 min, which represents a 97.8% recovery of silver in the solution.

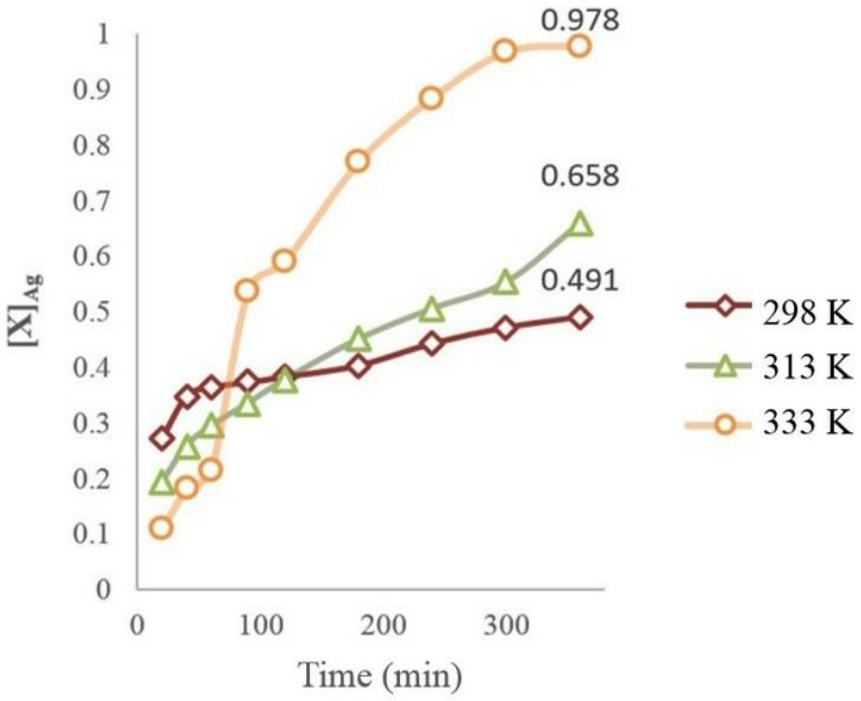

Figure 8. Representation of the effects on the leaching temperature of silver.

3.6. Identification of the Complexed Species of the Ag^+–$S_2O_3^{2-}$–O_2 System

Figure 9 reports the vibrations obtained from an individual leaching test under the following parameters: 0.5 L distilled water, 1 g electrolytic silver in the shape of shot, and 0.25 M thiosulfate in a glass reactor with magnetic stirring at 500 min^{-1}. The leaching had a duration of 24 h at 298 K in which a dissolution of 30% sample was achieved. The analysis performed on the leaching liquors of this test allow the typical vibrations corresponding to the formation of the thiosulfate ion ($S_2O_3^{2-}$) at wavelengths of 540 and 676 cm^{-1} were obtained. The vibrations of the species of $Ag(S_2O_3)_2^{3-}$ retained the same intensity when increasing the solution temperature from 298 to 333 K, as shown in Figure 10.

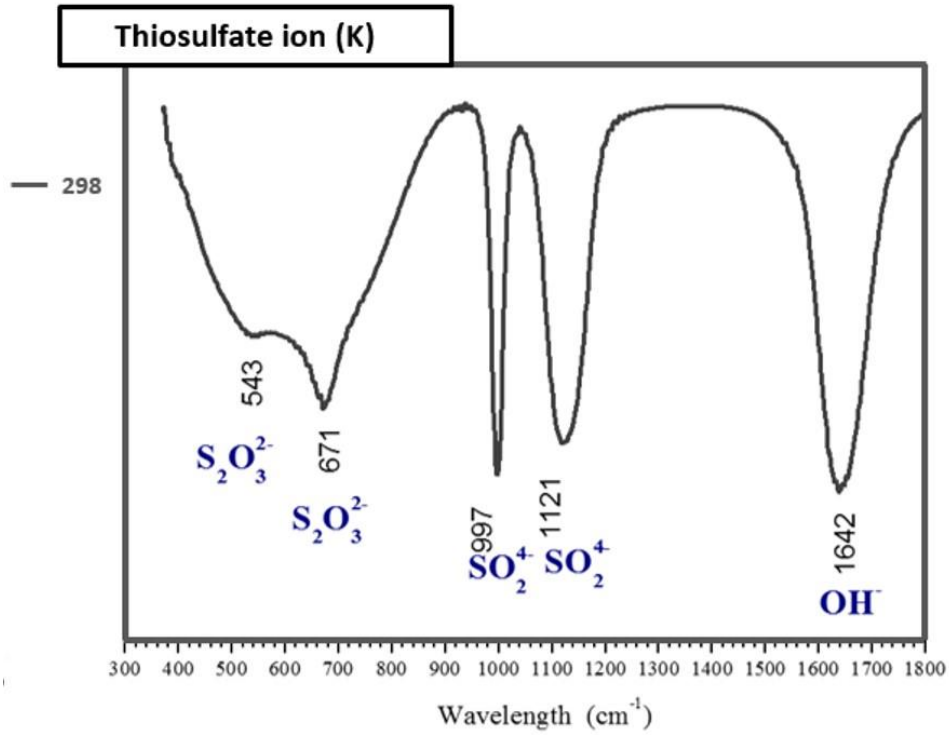

Figure 9. Infrared spectrum corresponding to thiosulfate ion at 298 K.

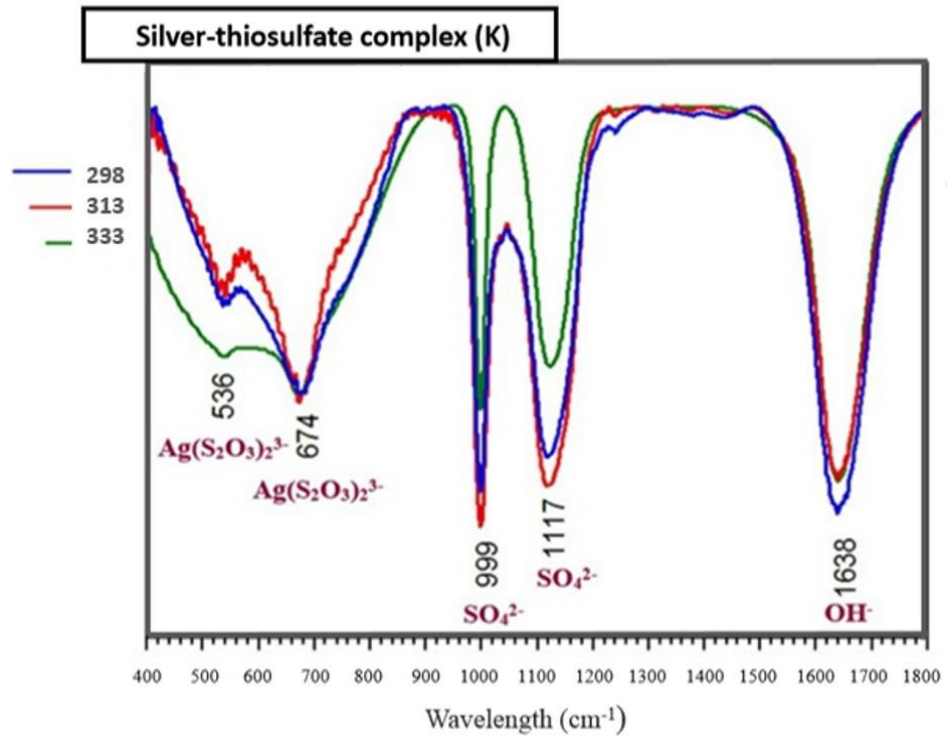

Figure 10. Infrared spectrum corresponding to silver thiosulfate at 298, 313, and 333 K.

4. Discussion

Figure 1 shows that the elemental weight of Zn in the mineral sample is 48%, qualifying the concentrate as a quality product for sale; however, the presence of multiple impurities such as Fe, Cu, and Ag make it a secondary source for the recovery of metals of interest. The concentrate of Zn was

obtained through a stepwise process of concentration, which is affected by the high content of Fe [8], which is reflected in the results obtained in the chemical analysis. The characterization performed by AAS reports an elemental content of 10.63% Fe, in addition to 1.97% Cu and 0.84% Pb. Elements such as Cd, Sb, As, and Ag are present in concentrations below 0.78%.

The Zimapán mining district is characterized by a varied and complex mineralogy, consisting primarily of sulphides and oxides, with significant outstanding metal concentrations, among which are elements such as Fe, Se, W, Zn, Cu, Pb, Cd, and Mo. The majority of the impurities in the mineral concentrate have place in the shape of sulphides, as is the case of Cu and Fe; which make up species as pyrite and chalcopyrite [9].

Said mineralogical phases were confirmed by elemental mapping carried out using SEM-EDS that is shown in Figure 5, wherein the relationship between particles with high content of S, Fe, and Cu is shown in addition to particles with right angles that were related with the typical crystal behavior of pyrite. Chalcopyrite is a complex nature species, which cannot be processed by traditional hydrometallurgical techniques such as cyanidation [10]; thus, the identification of this sulphur species in the concentrate of Zn is accurate, as it confirmed the diffractogram shown in Figure 2.

The higher concentration of silver (255 $g \cdot ton^{-1}$) was reported in the particles of the concentrate of Zn bounded to 74 microns, wherein arsenic content doubled the concentration of precious metal (541 $g \cdot ton^{-1}$). Silver is observed to be homogeneously distributed in the sample, as indicated by the chemical analysis of samples of concentrate of Zn delimited to differently sized particles. The study of these mineral deposits has allowed the confirmation of the formation of compounds where the sulfur combines with settleable elements such as As, Sb, or Bi, which relate to important contents of Ag, such as pyrargyrite (Ag_3SbS_3) and proustite (Ag_3AsS_3) [11]. The presence of As, Ag, and S in turn confirm mineralogical silver species identified by XRD.

Elements such as C, O, Fe, Zn, As, Al, Si, S, Ag, K, Ca, and Cu were identified in the EDS spectrum carried out to samples of powder particles bounded to 74 microns, which is shown in Figure 4 and has been associated to the elemental content reported in the mapping [12]. Figure 5 shows the results obtained by SEM mapping to non-metallic particles containing the elements forming species such as quartz (SiO_2), andradite ($Ca_3Fe_2(SiO_4)_3$), and orthoclase ($AlKSi_3O_8$), identified by XRD (spectrum not shown and published in a previous work [13]). The Ca content in the concentrate of Zn confirmed the alkaline nature of the pulp and corresponded to the presence of non-metal species such as calcite ($CaCO_3$) [14,15].

In order to establish an overview of the behavior which have the elements of the sample of the concentrate of Zn in contact with the leaching solution, the thermodynamic simulation of the $AgAsS_2$–$S_2O_3^{2-}$–H_2O system was performed in the temperature range from 298 to 333 K. Temperature shows no influence in the predominance areas of the species in the Ag–As–Na–S system; this is why only Pourbaix diagrams built with minor and major temperature parameters are shown. The oxidation of arsenic is carried out according to the Equations (1)–(3), wherein arsenic acid ($H_3AsO_4^{+}$) decomposes in dihydrogen-arsenate ($H_2AsO_4^{-}$), then to hydrogen-arsenate ($HAsO_4^{2+}$), and finally to arsenate (AsO_4^{3+}) [16] as pH increases (as shown in Figures 6 and 7).

$$H_3AsO_4 + H_2O = H_2AsO_4 + H_3O^+ \quad (1)$$

$$H_2AsO_4 + H_2O = HAsO_4^2 + H_3O^+ \quad (2)$$

$$AsO_4^2 + H_2O = AsO_4^3 + H_3O^+ \quad (3)$$

In the case of silver, it is shown that metal silver and silver sulfide are formed at reducing potentials. At oxidizing potentials (Eh > 0 V), the formation of the silver dithiosulfate species ($Ag(S_2O_3)_2^{3-}$) was reported, species which corresponds to the precious metal complex with leaching agent of the proposed system. At highly oxidizing potentials (Eh > 1.4 V) and alkaline pH, the silver precipitates in the shape of oxides.

The formation of silver-thiosulfate complex encompasses a wide range of pH within the limits of the water stability; however, it is important to consider the instability of the thiosulfate [17], because at temperatures over 338 K and under highly acid conditions, said factors may decrease the level of Ag complexation. This is why the experiments were performed at pH = 9 in an oxidizing media promoted by the injection of oxygen in the leaching solution in the established temperature range. The presence of the SO_4^{2-} ion and NaOH at pH = 9 at oxidizing potentials—which can be seen in both Pourbaix diagrams and vibrations obtained by FTIR—is due to dissolution and decomposition of the leaching agent $Na_2S_2O_3$ in aqueous system, which allows the formation of active thiosulfate ions.

Based on the species identified in the Pourbaix diagrams at pH = 9 and oxidizing conditions, the reaction stoichiometry dissolution was formulated using the proposed system, which is shown in Equation (4):

$$4AgAsS_2 + 6Na_2S_2O_3 + 8H_2O + 21O_2 + 28e^- = 4Ag(S_2O_3)_2^{3-} + 4HAsO_4^{2-} + 12NaOH + 4SO_4^{2-} \quad (4)$$

In previous work, the nature of heterogeneous reactions (solid–liquid) was studied, referring that the percent of conversion and the speed with which the reaction takes place show an important temperature dependence, suggesting a higher energy requirement for an efficient leaching process [18,19]. The results of the leaching tests at different temperatures that are seen in Figure 8 report high rates of silver conversion in solution with regard to the temperature increase, reaching a maximum dissolution of 97.8% Ag at 333 K.

The presence of the vibration bands in Figure 9 are consistent with those identified in the FTIR spectra of the leaching liquors of the mineral concentrate with thiosulfate [20]. In Figure 10 the presence of the thiosulfate ion contained in the leaching liquors at different temperatures is shown. The partial decomposition of thiosulfate ion ($S_2O_3^{2-}$) to sulfate (SO_4^{2-}) in basic medium is carried out in the presence of oxidizing agent [21], according to Equation (5).

$$S_2O_3^{2-} + 2O_2 + 2OH^- = 2SO_4^{2-} + H_2O \quad (5)$$

The tracking of the reaction of precious metal dissolution for all experiments was performed by AAS by checking the silver fraction in solution; thus, by these instrumental techniques, the formation of the silver-thiosulfate complex can be established.

5. Conclusions

- The species containing silver in Zn concentrate are silver-bearing sulfide arsenic ($AgAsS_2$), of which the reflections were identified by XRD and composition was confirmed by an exact analysis performed on fine particles using SEM-EDS.
- EDS microanalysis confirmed the presence of Cu, Zn, S, Fe, and Pb elements, the concentrations of which were analyzed using AAS. Micrographs obtained using SEM allowed the identification of the composition of typical ores, such as wurtzite (concentrate matrix), glance, and chalcopyrite, of which reflections were also observed in X-ray diffractograms.
- Using thermodynamic simulation of the dissolution of the species in the $S_2O_3^{2-}$-$AgAsS_2$-O_2 systems, it was found that a pH = 9 and Eh = 0 to 1.3 V is needed to obtain Ag (I) in solution at a temperature between 298 and 333 K, because potential minor species are generated as sulfides of silver arsenate and arsenic acid. This was confirmed by the experiments realized at different temperature ranges, where the formation of a silver complex was observed, even at high temperatures.

Author Contributions: Aislinn M. Teja-Ruiz designed and performed the experiments; Julio C. Juárez-Tapia conducted the discussion of results and wrote the paper; Leticia E. Hernández-Cruz realized the thermodynamic simulation of Ag (I) dissolution; Martín Reyes-Pérez performed the characterization by FTIR and contributed the software used for Thermodynamic Simulations; Francisco Patiño-Cardona performed the chemical analysis

and contributed to discussion of results; Ivan A. Reyes-Dominguez performed the characterization by DRX and mapping realized by SEM-EDS; Mizraim U. Flores-Guerrero realized the indexing of spectrum obtained by DRX; Elia G. Palacios-Baes performed the characterization by SEM-EDS.

Conflicts of Interest: The authors declare no conflicts of interest.

References

1. Syed, S. Silver recovery aqueous techniques from diverse sources: Hydrometallurgy in recycling. *Waste Manag.* **2016**, *50*, 234–256. [CrossRef] [PubMed]
2. Kholmogorov, A.; Kononova, O.; Danilenko, N.; Goryaeva, N.; Shatnykh, K.; Kachin, S. Recovery of silver from thiosulfate and thiocyanate leach solutions by adsorption on anion exchange resins and activated carbon. *Hydrometallurgy* **2007**, *88*, 189–195.
3. Alonso-Gómez, A.; Lapidus, G. Inhibition of lead solubilization during the leaching of gold and silver in ammoniacal thiosulfate solutions (effect of phosphate addition). *Hydrometallurgy* **2009**, *99*, 89–96. [CrossRef]
4. Aylmore, M.; Muir, D.M.; Staunton, W. Effect of minerals on the stability of gold in copper amoniacal thiosulfate solutions—The role of copper, silver and polythionates. *Hydrometallurgy* **2014**, *143*, 12–22. [CrossRef]
5. Juárez, J.; Rivera, I.; Patiño, F.; Reyes, M. Efecto de la temperatura y concentración de tiosulfatos sobre la velocidad de disolución de plata contenida en desechos mineros usando soluciones $S_2O_3^{2-}$–O_2–Zn^{2+}. *Inf. Technol.* **2012**, *23*, 133–138.
6. Briones, R.; Lapidus, G. The leaching of silver sulfide with the thiosulfate–ammonia–cupric ion system. *Hydrometallurgy* **1998**, *50*, 243–260. [CrossRef]
7. Deutsch, J.; Dreisinge, D. Lixiviación de Sulfuro de plata con tiosulfato en presencia de aditivos. Part I: Amoniaco-Cobre. *Hidrometallurgy* **2013**, *137*, 156–164. [CrossRef]
8. Moreno, R.; Téllez, J.; Fernández, M. Influencia de los minerales de los jales en la bioaccesibilidad de arsénico, plomo, zinc y cadmio en el distrito minero Zimapán. *Rev. Int. Contam. Ambient.* **2012**, *28*, 203–218. Available online: http://www.scielo.org.mx/scielo.php?script=sci_arttext&pid=S0188-49992012000300003 (accessed on 28 October 2015).
9. Xie, F.; Dreisinger, D.B. Use of ferricyanide for gold and silver cyanidation. *Trans. Nonferr. Met. Soc. China* **2009**, *19*, 714–718. [CrossRef]
10. González-Partida, E.; Carrillo-Chávez, A.; Levresse, G.; Tritlla, J.; Camprubı, A. Genetic implications of fluid inclusions in skarn chimney ore, Las Animas Zn–Pb–Ag(–F) deposit, Zimapán, México. *Ore Geol. Rev.* **2003**, *23*, 91–96. [CrossRef]
11. Solis-Marcial, O.J.; Lapidus, G.T. Chalcopyrite leaching in alcoholic acid media. *Hydrometallurgy* **2014**, *147–148*, 54–58. [CrossRef]
12. Labastida, I.; Armienta, M.A.; Lara-Castro, R.H.; Aguayo, A.; Cruz, O.; Ceniceros, N. Treatment of mining acidic leachates with indigenous limestone, Zimapan Mexico. *J. Hazard. Mater.* **2013**, *262*, 1187–1195. [CrossRef] [PubMed]
13. Reyes, M.; Perez, M.; Juárez, J.C.; Teja, A.M.; Patiño, F.; Flores, M.U.; Reyes, I.A. Characterization of a mineral of the district of Zimapan, Mina Concordia, Hidalgo, for the viability of the recovery of tungsten. In *Characterization of Minerals, Metals, and Materials 2016, Proceedings of the TMS 145th Annual Meeting and Exhibition, Nashville, TN, USA, 14–18 February 2016*; Ikhmayies, S.J., Li, B., Carpenter, J.S., Hwang, J.Y., Monteiro, S.N., Li, J., Firrao, D., Zhang, M., Peng, Z., Escobedo-Diaz, J.P., et al., Eds.; Springer: New York, NY, USA, 2016; pp. 547–554.
14. Foyo, A.; Tomillo, C.; Maycotte, J.I.; Willis, P. Geological features, permeability and groutability characteristics of the Zimapan Dam foundation, Hidalgo State, Mexico. *Eng. Geol.* **1997**, *46*, 157–174. [CrossRef]
15. Armienta, M.A.; Villaseñor, G.; Cruz, O.; Ceniceros, N.; Aguayo, A.; Morton, O. Geochemical processes and mobilization of toxic metals and metalloids in an As-rich base metal waste pile in Zimapán, Central Mexico. *Appl. Geochem.* **2012**, *27*, 2225–2237. [CrossRef]
16. Wua, D.; Sunb, S. Speciation analysis of As, Sb and Se. *Trends Environ. Anal. Chem.* **2016**, *11*, 9–22. [CrossRef]
17. Aylmore, M.G.; Muir, D.M. Thiosulfate leaching of gold—A review. *Miner. Eng.* **2001**, *14*, 135–174. [CrossRef]

18. Hernandez, J.; Patiño, F.; Rivera, I.; Reyes, I.A.; Flores, M.U.; Juárez, J.C.; Reyes, M. Leaching kinetics in cyanide media of Ag contained in the industrial mining-metallurgical wastes in the state of Hidalgo, Mexico. *Int. J. Min. Sci. Technol.* **2014**, *24*, 689–694. [CrossRef]
19. Rivera, I.; Patiño, F.; Roca, A.; Cruells, M. Kinetics of metallic silver leaching in the O_2-thiosulfate system. *Hydrometallurgy* **2015**, *156*, 63–70. [CrossRef]
20. Descostes, M.; Beaucaire, C.; Mercier, F.; Savoye, S.; Sow, J.; Zuddas, P. Effect of carbonate ions on pyrite (FeS_2) dissolution. *Bull. Soc. Geol. Fr.* **2002**, *173*, 265–270. [CrossRef]
21. Habashi, F. *Texbook of Hydrometallurgy*, 2nd ed.; Metallurgie Extractive: Québec City, QC, Canada, 1999; pp. 287–306.